

**Understanding the chemical bonding representation and the effect of
heteroatoms substitution in coronene**



*A thesis report submitted towards the partial fulfilment of
BS-MS Dual Degree Programme*

By
Anand Kumar
Reg. No. 20121009

Under the guidance of
Prof. Eluvathingal D Jemmis



Department of Inorganic and Physical Chemistry
Indian Institute of Science
Bangalore, India

Certificate

This is to certify that this dissertation entitled “**Understanding the chemical bonding representation and the effect of heteroatoms substitution in coronene**” towards the partial fulfilment of the BS-MS dual degree programme at the Indian Institute of Science Education and Research, Pune represents original research carried out by **Anand Kumar at Indian Institute of Science, Bangalore** under the supervision of **Prof. Eluvathingal D Jemmis**, Professor, Department of Inorganic and Physical Chemistry, Indian Institute of Science, Bangalore and **Prof. Miquel Solà**, Professor, Institut de Química Computacional i Catàlisi (IQCC), **Universitat de Girona, Girona, Spain** during the academic year 2016-2017.



Eluvathingal D Jemmis

Professor, Dept of Inorganic and
Physical Chemistry
Indian Institute of Science, Bangalore
560012, India
Phone +91 80 2293 3347
E-mail: jemmis@ipc.iisc.ernet.in



Miquel Solà

Professor, Institut de Química
Computacional i Catàlisi (IQCC),
Universitat de Girona, Girona, Spain
E-mail: miquel.sola@udg.edu

Date:

20-03-2017

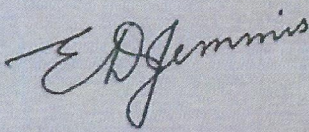
Declaration

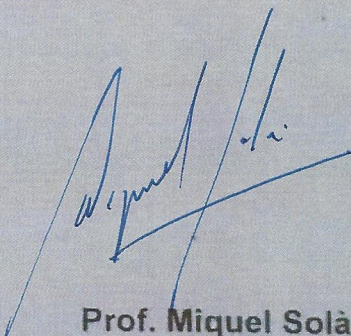
I hereby declare that the matter embodied in the report entitled "Understanding the chemical bonding representation and the effect of heteroatoms substitution in coronene" are the results of the investigations carried out by me at the Department of Inorganic and Physical Chemistry, Indian Institute of Science, under the supervision of Prof. Eluvathingal D Jemmis, Professor, Department of Inorganic and Physical Chemistry, Indian Institute of Science, Bangalore and Prof. Miquel Solà, Professor, Institut de Química Computacional i Catàlisi (IQCC), Universitat de Girona, Girona, Spain during the academic year 2016-2017 and the same has not been submitted elsewhere for any other degree.

Signature of Student

Anand 30/03/17
Anand Kumar

Signature of Thesis Supervisor


Prof. Eluvathingal D Jemmis


Prof. Miquel Solà

Dedicated to my Father

Acknowledgments

Once I began to write a few lines in this blank page, I realised that my stay at IISc Bangalore is about to be over. This long journey could not have been arrived at this stage without the support of several people.

First of all, I wish to express my sincere thanks and deepest gratitude to my supervisor **Prof. Eluvathingal D Jemmis** for his every suggestions which worked significantly, though in some cases I understood later. After working under him, I have learnt how to define and approach a scientific problem which is a rare and a lifelong experience to me. I am always amazed by his simplistic way of putting things. I am highly motivated by his excellent scientific efforts and enthusiasm towards the research and will remain in debt for his throughout support.

The journey of this work has started from Girona when I had an opportunity to visit **Prof. Miquel Solà** at University of Girona, Spain for my summer training. It has been a great privilege to work under his guidance. I extend my hearty thanks to him for motivating me constantly during my stay in Girona which led to partly accomplishment of present thesis. I am also very much thankful to **Dr. Jordi Poarter, Dr. Ferran Feixas** for helping me out of computational issues and helpful suggestions.

My special thanks goes to **Prof. Swapan K Ghosh** for his immense support right from my early days in undergraduation. I am very thankful to him for his timely meetings and philosophical sayings. I pass my best regards to my previous mentors, **Prof. Pratim K Chattaraj**, IIT Kharagpur and **Dr. Mahesh Sundararajan**, Theoretical Chemistry Division, Bhabha Atomic Research Centre, Mumbai who led me into the world of computational chemistry.

I must acknowledge **Dr. Arun Venkatnathan**, my local supervisor at IISER Pune for his valuable remarks. I would like to thank him for his valuable teaching during the computational chemistry course which has a direct association to my work

I owe my faith gratitude to all faculty members of the Chemistry Department at IISER Pune for their excellent and dynamic teaching during my academic program which has broadened my knowledge in the field of chemistry.

I have no words to express my profound appreciation to my present lab-mates, especially **Mr. Naiwrit Karmodak**, for their timely help in the neat execution of this project. I am overwhelmed by their inspiring guidance, pertinent criticism, pragmatic suggestions and extreme hospitality towards me. These aforementioned things applies to **Dr. Sudip Pan** too, who always remained by my side whenever I required. His dedication towards works always captivate me. I will extend my thanks to my lab mates Jyothish da, Sandeep da, Sagar da, Rinkumoni, Akhil, Shyama Chechi, Maruthu anna and Rahul da for making the proper amibience to work.

I would also like to thank all my friends Anupam da, Abhishek, Dinesh, KP, Anwesh, Pooja, Bappa da, Divya and many more for their extreme co-operation and providing a friendly atmosphere during the course of work.

Acknowledgments seem to be incomplete without a word of thanks to my **Maa, Gurudev, Jijaji** and family members whose blessings, co-operation, patience and prayers helped me to materialize my dream.

Above all, I thank **God Almighty** who enabled me with philosophy, perception and motivation to present this work.

Anand

Table of Contents

Table of Contents	3
Abstract	5
Chapter 1	6
Is coronene better described by Clar's aromatic π -sextet model or by the AdNDP representation?.....	6
[1.1] Introduction.....	6
[1.2] Computational Details	9
[1.2.1] Definition of Aromaticity:.....	10
[1.2.2] Structure-based aromatic descriptors – HOMA:.....	10
[1.2.3] Electron delocalization based aromatic descriptors – ESI:	11
[1.3] Results and Discussion	12
[1.4] Conclusions	19
Chapter 2	21
Modulation of structure, stability and aromaticity on step-wise BN pair substitution to coronene	21
[2.1] Introduction.....	21
[2.2] Computational Details	22
[2.3] Results and discussions.....	23
[2.3.1] Mono BN pair substitution:.....	23
[2.3.2] Double pair BN substitution:	28
[2.3.3] Triple pair BN substitution:.....	31
[2.4] Conclusion	34
[2.5] Future Direction	35
[2.5] References	35

Lists of Figure

Figure 1.1 Different representations of coronene.....	8
Figure 1.2 Clars and AdNDP representations of PAHs	12
Figure 1.3 Bond lengths of PAHs.....	14
Figure 1.4 NICS-X-Scan of coronene	16
Figure 2.1 Numbering scheme of Coronene	24
Figure 2.2 Five most stable single BN substituted coronene	25
Figure 2.3 NBO charges of unsubstituted coronene.....	27
Figure 2.4 Five most stable double BN substituted coronene	28
Figure 2.5 NBO charges of single BN substituted coronene	29
Figure 2.6 Five most stable triple BN substituted coronene	32
Figure 2.7 NBO charges of double substituted coronene	33

List of Tables

Table 1.1 Aromaticity values of PAHs.....	17
Table 1.2 Energetics values of PAHs.....	18
Table 2.1 Relative energy, aromaticity for single substituted coronene.....	27
Table 2.2 Relative energy, aromaticity for double substituted coronene.....	30
Table 2.3 Relative energy, aromaticity for triple substituted coronene.....	34

Abstract

The bonding patterns in coronene are complicated and controversial. Among the different proposed descriptions, the two most representative are those generated by Clar's aromatic π -sextet and Adaptive Natural Density Partitioning (AdNDP) models. The chapter 1 reports the detailed quantum-chemical calculations at the density functional theory level to evaluate the model that gives a better representation of coronene. In addition, the analysis of the molecular structure of coronene, quantification of the aromaticity using various local aromaticity descriptors and assessment of the Diels-Alder reactivity with cyclopentadiene have been carried out. It has been concluded that Clar's π -sextet model provides the representation of coronene that better describes the physicochemical behaviour of this molecule.

The recent studies show that properties of coronene could be tuned by isoelectronic substitution procedures. Thus, the effect of single, double and triple BN pair substitution on the aromaticity and stability of coronene is investigated in Chapter 2. The nucleus-independent chemical shift (NICS)-based method, has been used for its aromaticity assessment. The study reveals that the positional isomers with adjacently placed BN units are the most stable structure. Charge separation and different bond strength together play an important role in rationalizing the relative stability trends. The aromatic character of all BN substituted rings decreases w.r.t unsubstituted coronene except in case of triple BN pair substitution in inner ring, where the $\text{NICS}_{zz}(1)$ values of outer rings increase. It is found that depending upon the position of BN pairs, the HOMO-LUMO gap of coronene could be modulated. Thus, it is proposed to study the opto-electronic properties of these molecules.

Chapter 1

Is coronene better described by Clar's aromatic π -sextet model or by the AdNDP representation?

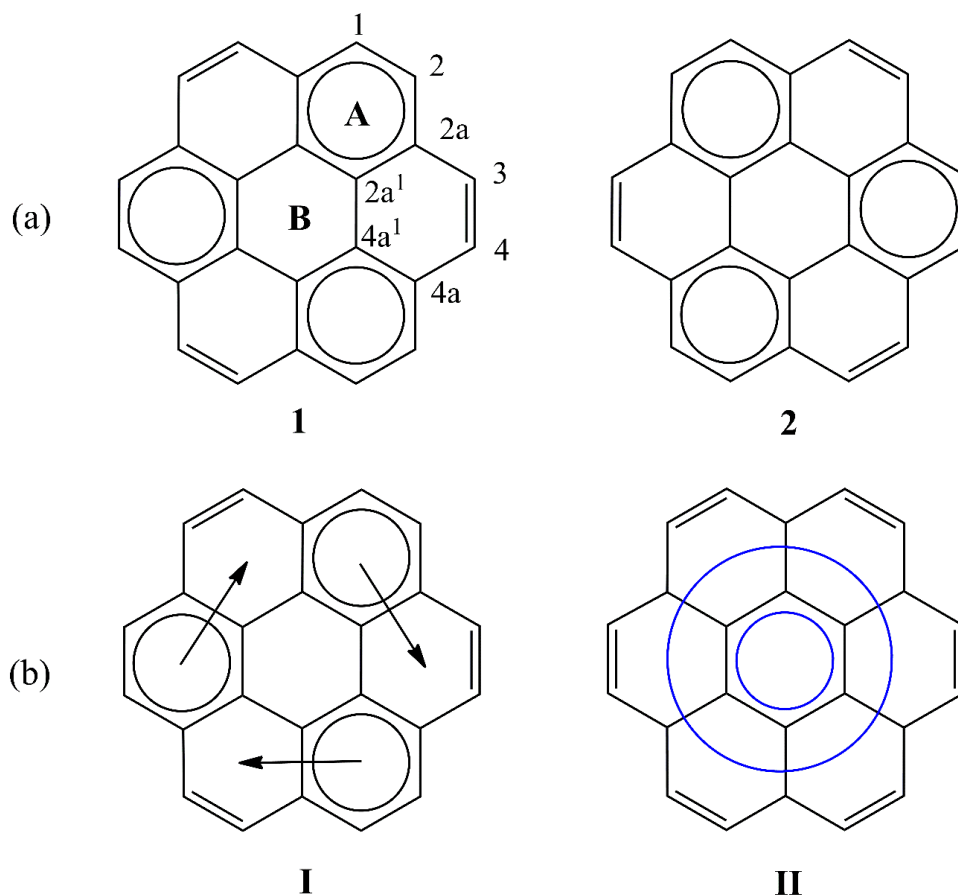
[1.1] Introduction

Aromaticity is one of the most distinguished concepts in physical organic chemistry. It is crucial for understanding the geometry, stability, spectroscopy, and chemical reactivity of a considerable number of molecules.¹ In 1931, Hückel laid the stepping stone by proposing the acclaimed Hückel's $4n + 2$ rule to identify aromaticity in annulenes.² Since the applications of Hückel's $4n + 2$ rule were limited to monocyclic conjugated systems, several trials were performed to generalize this rule to polycyclic systems. Amongst them, one of the most prominent model was Clar's aromatic π -sextet rule,³ which claims that the Kekulé structure with the largest number of disjoint aromatic π -sextets, i.e. the so-called Clar valence structure, is the one that offers the best description of benzenoid polycyclic aromatic hydrocarbons (PAHs). This model was extended by Glidewell and Lloyd⁴ to polycyclic conjugated hydrocarbons having rings with any even number of carbon atoms in their structure.⁵ Several studies among the years provided support to Clar's π -sextet model.⁶ More recently, Zubarev and Boldyrev⁷ developed the Adaptive Natural Density Partitioning (AdNDP) method as an improvement of the Natural Bond Orbital (NBO)⁸ analysis. In the AdNDP approach, the charge density is partitioned into n -center 2-electron bonds (nc -2e) with the highest possible degree of localization of electron pairs. In this manner, AdNDP recovers both Lewis bonding elements (1c-2e and 2c-2e objects, corresponding to the core electrons and lone pairs, and 2c-2e bonds) and delocalized bonding elements, which are associated with the concepts of multicenter bonding and aromaticity. AdNDP is a very efficient and visual method to analyse molecular orbital-based wave functions. This method has successfully described the chemical bonding patterns in several molecular clusters with many delocalized bonds providing interesting information and deep insight.⁹ Interestingly, for PAHs that can be described with a unique Clar valence structure (for instance,

phenanthrene, triphenylene, or circumcoronene), the description of the chemical bonding given by Clar's π -sextet model and the AdNDP approach coincide.¹⁰ On the contrary, for PAHs described by a combination of several Clar valence structures (for instance, naphthalene, anthracene, or coronene), the two representations disagree. The discrepancy is attributed to the fact that the AdNDP analysis looks for the most compact *single* structure that can be used to define chemical bonding in a certain compound whereas Clar's π -sextet model uses a resonant description of the chemical bond.¹⁰

Hexabenzobenzene or coronene ($C_{24}H_{12}$) is one of the PAHs in which the chemical bonding pattern described by Clar and AdNDP models¹⁰ differ. This benzenoid PAH with applications in materials chemistry,¹¹ comprises six benzene rings annelated to a benzene core and represents a basic graphene fragment. It is found naturally as a mineral called carpathite and is produced in hydrocracking petroleum-refining process.¹² Although initially it was considered coronene as a superaromatic compound,¹³ it is now widely accepted that it is not.¹⁴ In fact, the aromatic stabilization energy (ASE) of coronene per π -electron was found to be significantly lower than that of pyrene that, in turn, is much lower than that of benzene. Coronene structure can be represented by 20 covalent resonance structures, two of them having three π -sextets and D_{3h} symmetry (structures **1** and **2** in Figure 1.1). The Clar valence structure, which is a combination of the two D_{3h} resonant structures with three π -sextets, has D_{6h} symmetry with three π -sextets that can migrate into the adjacent rings (structure **I**, Figure 1.1). Therefore, one can consider that each outer ring of coronene has half a π -sextet, whereas no π -sextet is located in the inner 'empty ring'. On the other hand, according to the AdNDP model,¹⁰ the 108 valence electrons of coronene are distributed in 30 2c-2e C–C bonds, 12 2c-2e C–H bonds, six 2c-2e π bonds, three 6c-2e π bonds, and three 24c-2e π bonds (structure **II**, Figure 1.1). In the AdNDP representation, the π -system coronene is reminiscent to that of the B_{19}^- species,¹⁵ an aromatic Wankel motor¹⁶ with double-aromaticity in two concentric-systems.

Figure 1.1. (a) The two out of 20 covalent resonant structures of coronene having three π -sextets (b) The two different representations of coronene molecule according to the Clar (**I**) and AdNDP (**II**) models.



The estimated local properties of coronene differ considerably depending on which representation one considers. For instance, bond C1–C2 should be in between intermediate and double bond somewhat closer to double bond in Clar's representation, whereas it should have slightly more than double bond character in the AdNDP model. Similarly, the aromaticity of the outer ring **A** (Figure 1.1) should be larger than that of the inner ring **B** in the Clar model and the other way round according to the AdNDP representation. In the present work, we investigate the best-suited model between Clar's aromatic π -sextet and AdNDP forms for representing coronene. To this end, we have analysed the molecular structure, aromaticity, and reactivity of coronene as compared to that of naphthalene and phenanthrene. We

agree with Kutzelnigg who said:¹⁷ “Understanding without models is impossible. However, a model is useful, only if one understands its scope and limitations.” In this sense, we think it is worth to look for possible shortages of these models keeping in mind that models are just intrinsically deficient approximations to reality and that there is no perfect model. However, when comparing different models the degree of approximation to reality can be different and it is relevant to know which is the model that better approaches it and, consequently, is more useful. As Dewar wrote:¹⁸ “the only criterion of a model is usefulness, not its “truth””. In the current study, a rational attempt has been made in order to conclude the foremost representation between the Clar’s and the AdNDP models of coronene.

[1.2] Computational Details

All considered geometries were optimized using hybrid density functional theory (DFT) with the M06-2X¹⁹ and B3LYP²⁰ methods in conjunction with the cc-pVTZ Dunning type basis set.²¹ Grimme’s-D3 dispersion correction²² with the Becke-Johnson (BJ) damping²³ was included in all B3LYP calculations. These two functionals perform quite well for the predicting relative energies of polycyclic aromatic hydrocarbons.²⁴ Harmonic vibrational frequencies were performed to characterize the nature of stationary points and to obtain enthalpies and Gibbs energies. The reported minima and transition states structures exhibited zero and one imaginary frequencies, respectively. All geometry optimizations and frequency calculations were carried out using the Gaussian 09 set of programs.²⁵ Following previous recommendations,²⁶ the local aromaticity in the systems considered was studied using several aromaticity indices like the geometric-based²⁷ harmonic model of aromaticity (HOMA),²⁸ the electronic-based²⁹ *para*-delocalization index (PDI),³⁰ aromatic fluctuation index (FLU),³¹ Giambiagi’s index (I_{ring}),³² and multicentre index (MCI),^{14f} and the magnetic-based³³ nucleus-independent chemical shift (NICS).³⁴ The NICS was evaluated using the regular GIAO method³⁵ on probing ghost atoms at the ring centres and to 1.0 Å away from the ring centre following the perpendicular of the molecular plane. We also performed NICS-XY-scans.^{33d, 36} These scans can distinguish the global (current along the perimeter of whole molecule) and local

(current inside each circuit) currents in π -conjugated polycyclics. The NICS-XY-scans were recorded using NICS_{zz} values at 1.7 Å above the molecular plane at the M06-2X/cc-pVTZ computational level. As to the aromaticity indices calculated, the aromaticity of a given ring increases when HOMA, PDI, I_{ring}, and MCI increase and FLU and NICS decrease. All electronic indices of aromaticity were obtained with the ESI-3D program^{31, 37} using overlaps of molecular orbitals generated by the AIMALL program³⁸ and calculated with the Atoms-in-Molecules atomic partition.³⁹

[1.2.1] Definition of Aromaticity:

Schleyer and coworkers proposed the following definition:

"Aromaticity is a manifestation of electron delocalization in closed circuits, either in two or in three dimensions. Since it is not an observable property, aromaticity is measured from its multiple manifestations. The most common aromaticity descriptors are those based on structural parameters, energetic criteria, magnetic properties, reactivity indices, or electron delocalization measures. Herein, we have briefly explained the various aromatic descriptors.

[1.2.2] Structure-based aromatic descriptors – HOMA:

The structural aromaticity descriptors are based on the idea that the tendency toward bond length equalization and the symmetry of the ring are important manifestations of aromaticity. Among the most common structural-based measures, the harmonic oscillator model of aromaticity (HOMA) index²⁸ defined by Kruszewski and Krygowski has proven to be one of the most effective structural indicators of aromaticity:

$$\text{HOMA} = 1 - \frac{\alpha}{n} \sum_{i=1}^n (R_{\text{opt}} - R_i)^2 \quad (1.1)$$

where n is the number of bonds considered and α is an empirical constant (for C-C, C-N, C-O, and N-N bonds $\alpha=257.7, 93.5, 157.4,$ and $130.3,$ respectively) fixed to give HOMA= 0 for a model nonaromatic system and HOMA=1 for a system with all bonds equal to an optimal value R_{opt} , assumed to be achieved for fully aromatic systems. R_i stands for the running bond length. The HOMA value can be decomposed into the energetic (EN) and geometric (GEO) contributions according to the next relation: 164

$$\text{HOMA} = 1 - \text{EN} - \text{GEO} = 1 - \alpha(R_{\text{opt}} - \bar{R})^2 - \frac{\alpha}{n} \sum_i (\bar{R} - R_i)^2 \quad (1.2)$$

The GEO contribution measures the decrease or increase in bond length alternation while the EN term takes into account the lengthening/shortening of the mean bond lengths of the ring.

[1.2.3] Electron delocalization based aromatic descriptors – ESI:

First, the *para*-delocalization index (PDI), is local aromatic indicator, derived from delocalization index (DI) as structured in the AIM theory of Bader. The PDI is an average measurement of electron delocalization among three *para*-related positions exist in a 6-MR ring. Let us assume that the ring structure consists of n atoms which is defined by the string $A = [A_1, A_2, \dots, A_n]$, where each element is ordered according to the connectivity of the atoms in the ring. According to definition, the PDI of a six membered ring is given by:

$$\text{PDI}(A) = \frac{\delta(A1,A4)+\delta(A2,A5)+\delta(A3,A6)}{3} \quad (1.3)$$

It is found worthy when it comes to polycyclic system like PAHs, fullerenes or nanotubes. However, the PDI is confined to six members ring by definition and we cannot evaluate it for ring structure having lone-pairs containing atoms. To improve this theory, two years later, Matito, Duran, and Solá (MDS)³⁰ proposed a new methodology, the aromatic fluctuation index, FLU which is applicable to any ring size. The key idea behind FLU indicator is that the aromaticity is not only related to electron sharing but also with the atomic delocalization of π -electron. Hence, it accounts for the consistency of electron delocalization along the ring and its electron sharing difference between the adjacent atoms with respect to aromatic reference, and it is given by:

$$\text{FLU}(A) = \frac{1}{n} \sum_{i=1}^n \left[\left(\frac{\delta(A_i)}{\delta(A_{i-1})} \right)^\alpha \left(\frac{\delta(A_i, A_{i-1}) - \delta_{\text{ref}}(A_i, A_{i-1})}{\delta_{\text{ref}}(A_i, A_{i-1})} \right) \right]^2 \quad (1.4)$$

where $A_0 \equiv A_n$, $\delta_{\text{ref}}(A_i, A_{i-1})$ is taken from an aromatic molecule, for example, for C-C bonds, benzene is considered as reference and the atomic delocalization is defined as:

$$\delta(A_i) = \sum_{A_i \neq A_j} \delta(A_i, A_j), \quad (1.5)$$

And α is a general function to make sure that the first term in the equation (1.4) is always greater or equal to 1,

$$\alpha = \begin{cases} 1 & \delta(A_i) > \delta(A_{i-1}) \\ -1 & \delta(A_i) \leq \delta(A_{i-1}) \end{cases} \quad (1.6)$$

The FLU value close to 0 signifies the system is aromatic and it increases as the system becomes non-aromatic. This aromatic descriptor is heavily related to the reference and hence it cannot be employed to investigate reactivity.

[1.3] Results and Discussion

Figure 1.2 illustrates the Clar and AdNDP representations of naphthalene and phenanthrene and the Clar model of pyrene. The latter PAH has a unique Clar valence structure and, therefore, it is likely that AdNDP provides the same description as the Clar model. Naphthalene, phenanthrene, and pyrene can be considered fragments of coronene with different bonding patterns. We will compare the molecular structure, aromaticity, and reactivity of these fragments with those of coronene to discuss whether coronene is better described by Clar or AdNDP representations. We will focus our comparisons on naphthalene and phenanthrene. The results of pyrene, having a similar bonding pattern as phenanthrene are given in the Supporting Information (SI).

This section is organized as follows. First, we discuss the molecular structure of coronene, second, we analyse the local aromaticity of the inner and outer ring of coronene, and, finally, we study the reactivity of coronene in Diels-Alder reactions.

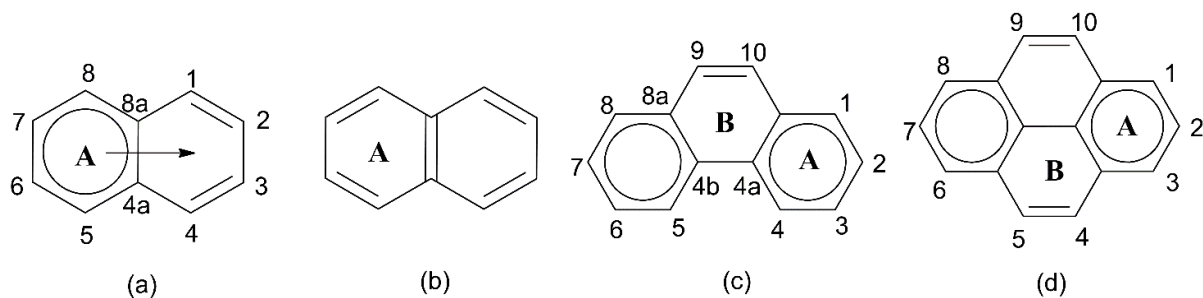


Figure 1.2 (a) The Clar representation of naphthalene, (b) the AdNDP model of naphthalene, (c) the representation of phenanthrene according to AdNDP and Clar models, and (d) the Clar representation of pyrene.

a. The molecular structure of coronene.

Root-mean-square deviations (RMSDs) of theoretical bond lengths for the two distinct DFT levels with respect to experimental values of Figure 1.3 indicate similar accuracy for the M06-2X/cc-pVTZ (RMSD = 0.060 Å) and B3LYP/cc-pVTZ (RMSD = 0.062 Å) levels of theory

$$RMSD = \sqrt{\frac{1}{n} \sum_{i=1}^n \left(R_i - R_{\text{exp}} \right)^2} \quad (1.7)$$

We have decided to focus our comments on the M06-2X/cc-pVTZ results and move the B3LYP/cc-pVTZ results to the SI. The conclusions extracted from the B3LYP/cc-pVTZ results are the same as those derived from the M06-2X/cc-pVTZ calculations. Figure 1.3 gives the bond lengths of naphthalene, phenanthrene, pyrene, and coronene. According to the AdNDP representation, the short outer C1–C2 bond (Figure 1) in coronene has a bond order of 2.1 (2c-2e σ bond, 2c-2e π bond, and three 24c-2e π bonds; for these latter we consider the three electron pairs equally distributed among the 30 bonds of coronene). On the contrary, the Clar description considers that the bond order of the C1–C2 bond in coronene is 1.75. Figure 1.3 shows that the C9–C10 double bond in phenanthrene (1.348 Å, exp. 1.341 Å⁴¹) has a shorter bond length than the C1–C2 bond of coronene (1.362 Å, exp. 1.357 Å⁴²). Clar’s description conforms better this experimental observation. Moreover, the long outer C2–C2a bond in coronene should have a bond order of 1.1 and 1.25 according to the AdNDP and Clar models. Similarly, the bond order of the central C2a¹–C4a¹ bond in coronene is 1.6 and 1.25 in the AdNDP and Clar representations, respectively. And the spoke C2a¹–C2a predicted bond orders are 1.1 and 1.5 in the AdNDP and Clar description. Therefore, AdNDP predicts the central C2a¹–C4a¹ bond (1.421 Å, exp. 1.424 Å) to be shorter than the spoke C2a¹–C2a bond (1.408 Å,

exp. 1.416 Å), whereas Clar's model indicates the contrary. Experimental values favour the expectation of Clar's model. In addition, Clar's model predicts similar bond lengths for the long outer C2–C2a bond (1.419 Å, exp. 1.420 Å) and the central C2a¹–C4a¹ bond (1.421 Å, exp. 1.424 Å) as found experimentally, whereas AdNDP indicates shorter central than outer bond length. Finally, the fact that the spoke C2a¹–C2a bond of coronene (1.408 Å, exp. 1.416 Å) is closer to the C4–C4a of naphthalene (1.415 Å, exp. 1.425 Å) than to the C8a–C9 of phenanthrene (1.434 Å, exp. 1.450 Å) supports the conclusion that, geometrically, the outer rings of coronene are more similar to the rings of naphthalene than to the central ring of phenanthrene, thus favouring Clar's representation.

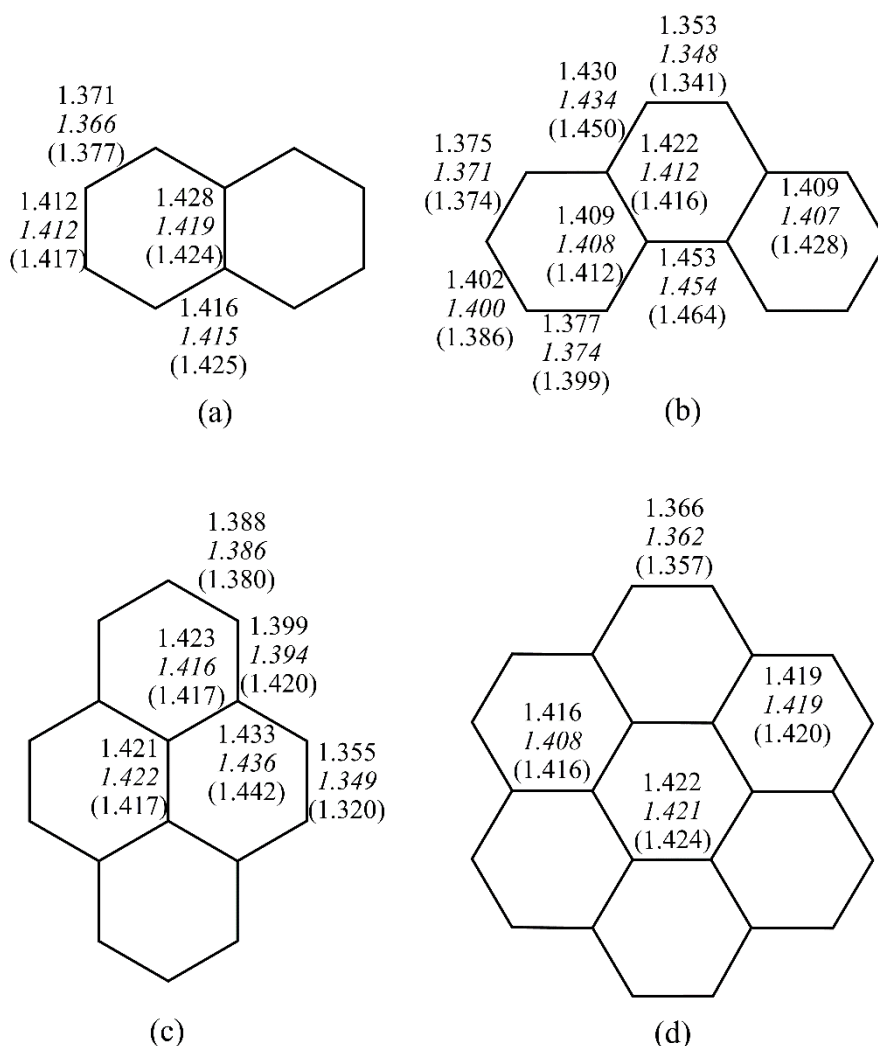


Figure 1.3. B3LYP/cc-pVTZ, M06-2X/cc-pVTZ (in italics), and experimental (in parentheses) bond lengths (in Å) of (a) naphthalene (experimental values from ref.40

a), (b) phenanthrene (experimental values from ref.40 b), (c) pyrene (experimental values from ref.41), and (d) coronene (experimental values averaged considering D_{6h} symmetry from ref.42).

b. The local aromaticity of coronene.

In the AdNDP model, the inner ring of coronene is expected to be more aromatic than outer ring. On the contrary, Clar's π -sextet scheme suggests the local aromaticity of the outer ring to be larger than that of the inner ring. Table 1.1 collects FLU, PDI, MCI, I_{ring} , NICS(1)_{zz}, and HOMA values of the investigated PAHs. All indices agree indicating that the outer ring **A** is more aromatic than the inner ring **B**. HOMA is the index showing the smallest difference between the two rings. In addition, HOMA is the only index that considers ring **B** of coronene more aromatic than that of phenanthrene. These results seems to indicate that HOMA overestimates the aromaticity of ring **B** of coronene. On the other hand, NICS(1)_{zz} is the indicator providing the largest dissimilarity between rings **A** and **B** of coronene. As it is well-known, in fused polycyclic conjugated hydrocarbons, NICS measure is affected by the couplings between induced magnetic fields generated by adjacent rings.⁴³ In fact, it has been already suggested that the NICS value of the inner ring of coronene is underestimated and it should be more negative.¹⁹ We also calculated the NICS-X-scan for the different species (see Fig. 1.1 for coronene and Fig. S2 for the rest of species studied). Results of the NICS-X-scan also points out that the outer ring is the most aromatic in coronene. Not only the indices used in this work, but also other indices used in previous works like NICS(0),¹⁰ NICS(1),⁶ NICS(0)_{zz},¹⁰ NICS(0) _{π zz},⁴⁵ SSE, BOIA,¹⁴ as well as FLU, PDI, and MCI calculated with the Hückel molecular orbital method⁴⁶ point in the same direction. In addition, the topography of the molecular electrostatic potential of coronene⁴⁷ strongly support the Clar's model that describes the innermost ring of coronene as an 'empty ring'. The only index that gives a large aromaticity for the central ring is the extra cyclic resonance energy (ECRE) that indicates the inner ring of coronene to have similar aromaticity than benzene.⁴⁵ In summary, the outer ring of coronene is more aromatic than the inner ring and this result is in accordance with Clar's model prediction. This conclusion agrees with Scanning Tunnelling Microscope (STM) images that show coronene as a hollow ring like structure with a circular protrusion for the outer rings of coronene and

a small depression for the central 'empty ring'.⁴⁸ Finally, all indices in Table 1.1 except NICS(1)_{zz}, consider that the aromaticity of the outer ring of coronene is closer to that of the ring of naphthalene than to that of the outer ring of phenanthrene and that the aromaticity of the inner ring in coronene is similar (but somewhat lower except in the case of HOMA) to that of the central ring in phenanthrene.

Figure 1.4 M06-2X/cc-pVTZ NICS-X-scan of coronene performed at a height of 1.7 Å. The scheme of the considered axis is shown next to the NICS plot.

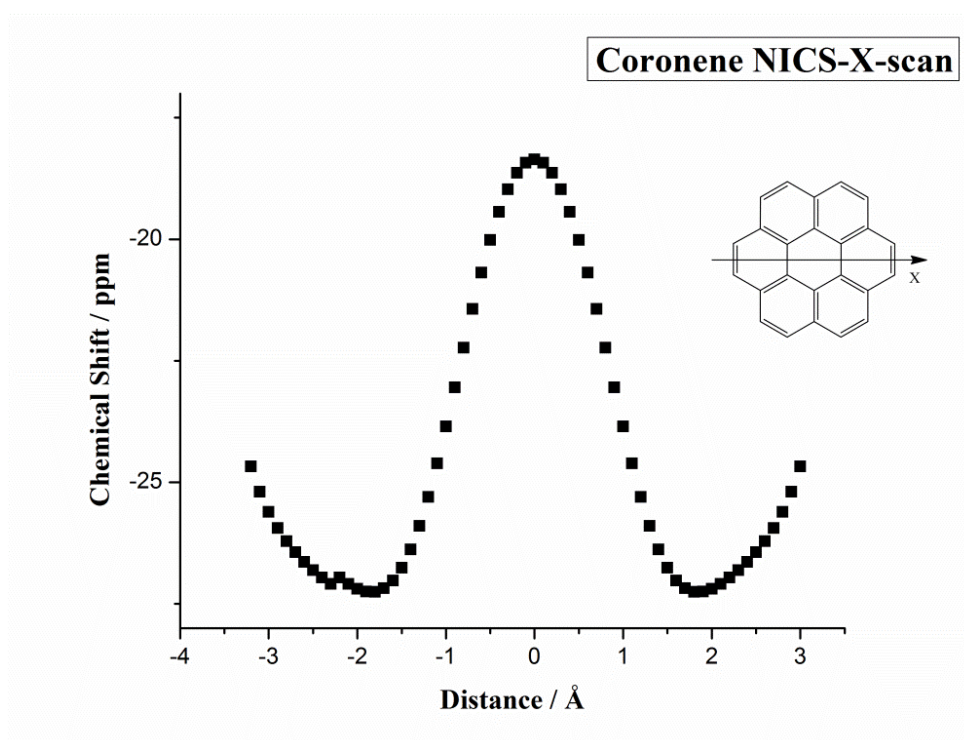


Table 1.1. M06-2X/cc-pVTZ values of PDI, MCI, and I_{ring} (in electrons), FLU, HOMA, and NICS (in ppm) for the investigated PAHs (see Figures 1.1 and 1.2 for ring labels).

Indices	Ring	Naphthalene	Phenanthrene	Coronene
PDI	A	0.076	0.083	0.055
	B		0.047	0.030
FLU	A	0.010	0.005	0.013
	B		0.022	0.020

MCI	A	0.038	0.047	0.024
	B		0.017	0.011
I_{ring}	A	0.027	0.033	0.018
	B		0.013	0.009
HOMA	A	0.830	0.917	0.808
	B		0.519	0.716
NICS(1) _{zz}	A	-30.42	-30.50	-32.42
	B		-20.85	-6.46

The ring currents of coronene were computed in previous works using different approximations.^{6, 49} These studies showed the presence of a diamagnetic ring current in the [18]annulene periphery and a weak paramagnetic ring current in the central six-membered ring. This pattern of ring currents was interpreted as the result of a combination of diamagnetic local ring currents in all six-membered rings.^{6, 14} This combination also explains the lack of radial currents. Moreover, considering the intensity of the outer rings being two or three times stronger than that of the inner ring, the observed global pattern of counter-rotating strong rim and weak hub currents in coronene is perfectly reproduced.^{6, 14} A more intense diamagnetic local ring current in the outer rings concurs with the larger aromaticity attributed to these rings as compared to the inner ring by all indices of aromaticity. This picture of local ring currents is analogous to that derived from the Clar's model. In the AdNDP representation, we have a 6π (i.e, $4n+2$) inner circuit with three $6c-2e$ π bonds and another 6π circuit in the periphery with three $24c-2e$ π bonds. Since the two circuits have 6π electrons, one should observe two (inner and outer) diamagnetic ring currents.

In summary, many descriptors of aromaticity points out that the outer rings of coronene are more aromatic than the central ring. In addition, the ring currents show a diamagnetic ring current in the [18]annulene rim and a weak paramagnetic ring current in the [6]annulene inner perimeter. These observations are more in line with expectations from Clar's model than from the AdNDP representation.

c. *The reactivity of coronene.*

In this last section, we study the Diels-Alder (DA) reaction between the analysed PAHs and cyclopentadiene. We calculated the endo and exo approaches for the DA, although in Table 2 we gather only the results for the thermochemistry and kinetics of the exo approach, which is the most favourable approach for most of the systems studied. However, the results of the endo approach are also provided in the SI. The DA reaction has been studied on the C1–C2 bond of coronene, the C9–C10 bond of phenanthrene, and the C1–C2 bond of naphthalene. As before, we consider that the reactivity of the C1–C2 bond in coronene has to be more similar to that of C9–C10 bond in phenanthrene if the AdDNP representation is followed and to that of C1–C2 bond of naphthalene according to the Clar description.

Table 1.2. M06-2X/cc-pVTZ values of reaction energies and energy barriers for the investigated PAHs. Enthalpies and Gibbs energies in kcal mol⁻¹.

Compound	Bonds ^a	ΔH_r	ΔG_r	ΔH^\ddagger	ΔG^\ddagger
Naphthalene	C1–C2	1.00	14.57	30.62	35.65
Phenanthrene	C9–C10	-3.78	10.15	27.93	32.32
Coronene	C3–C4	0.35	13.29	30.53	35.02

^a Labels of C atoms in Figures 1.1 and 1.2.

Values of Table 1.2 indicate that the most and least reactive bonds are those of phenanthrene and naphthalene, respectively. The reaction energy and energy barriers of the C1–C2 bond in coronene differ by less than 0.7 kcal mol⁻¹ from those of the C1–C2 bond of naphthalene, whereas differences are larger than 2.5 kcal mol⁻¹ when compared to those of the C9–C10 bond in phenanthrene. Hence, this reactivity analysis shows coronene being more 'naphthalene-like' than 'phenanthrene-like', thus emphasizing Clar's model as a prime representation of coronene. Finally, results in Table 1.2 clearly show that coronene cannot undergo

Diels-Alder reactions in the C1–C2 bond because of the high barrier and endergonic nature of the reaction.

As a whole, analysis of the molecular structure, aromaticity, and reactivity indicates that the Clar representation of coronene describes better its bonding pattern than the AdNDP model. This view is also supported by ring currents calculations and STM images of coronene. We attribute the failure of AdNDP to provide a better representation of coronene to the fact that AdNDP by construction looks for the single most compact description avoiding a resonant description of the chemical bond. We argue that PAHs that are described in Clar's π -sextet model with Clar valence structures having π -migrating sextets, are not well-represented by a single structure. In fact, if threshold for acceptance of 2c-2e bonds in the AdNDP analysis is reduced to 1.55 e, the AdNDP method recovers a Kekulé structure like **1** in Figure 1.1.¹⁰ It is likely that if resonance were introduced in AdNDP analysis, the result would be a combination of structures **1** and **2** in Figure 1.1, i.e., the same representation given by Clar's theory. Finally, although we consider that, for coronene, the representation given by Clar's method is better than that provided by the AdNDP approach, it is important to emphasize that Clar's model is restricted to benzenoid PAHs, whereas AdNDP can be applied to any chemical system.

[1.4] Conclusions

The representation of the bonding pattern in coronene is complicated and controversial. In the present work, we compare the descriptions of this molecule given by Clar's π -sextet model and the Adaptive Natural Density Partitioning (AdNDP) method, the aim being to find the best representation of the bonding in coronene. To this end, we analyse the molecular structure, the local aromaticity, and the local chemical reactivity of coronene as a dienophile in a Diels-Alder reaction with cyclopentadiene. Keeping in mind that any model of the bonding pattern is intrinsically deficient as it makes approximations, the results obtained favour the Clar representation as the best suited to describe the chemical bond in coronene. We attribute the possible origin of the shortcoming of AdNDP when applied to coronene to the need of including resonant structures in the description of this molecule.

Chapter 2

Modulation of structure, stability and aromaticity on step-wise BN pair substitution to coronene

[2.1] Introduction

The heteroatom substitution of carbon atoms in graphene is an effective way to modulate its properties and applications.⁵⁰ Due to presence of heteroatoms, delocalized bonding picture and aromaticity are distorted.⁵¹ This engineers the energy of the frontier bands and give rise to several interesting properties in graphene. The PAHs are subsets of this extended system, where the delocalization of the π -electron density influence much of its chemistry. The aromatic analysis of coronene, as shown in the previous chapter, gives an overview of the π -electron framework present in coronene and its reactivity towards diene. In this chapter, we further confirm the aromatic characteristics of coronene and the most probable representation of the C-C double bonds using the criterion of heteroatom substitution. One of the prominent strategy to substitute the C=C bonds is with the isoelectronic BN pairs, which modulate the chemical properties leaving the geometry almost unaltered.⁵² Though the electronegativities of B and N differs from carbon, the average value along the BN bond almost coincides with that of the C-C bond. Let us begin with the smallest aromatic ring, benzene to understand the effect of BN substitution on its electronic structure. The substitution of the C-C bonds with BN pairs reduces the electronic delocalization throughout the framework due to the localized bonding in BN pair. Thus the HOMO-LUMO gap is altered depending upon the number of C-C bonds substituted with BN. While the mono BN substitution reduces the gap, in borazine the gap is increased w.r.t benzene.⁵³ Although for benzene the tuning of HOMO-LUMO gap do not found to bring much alternation its properties, but the idea influenced the study of effect of BN substitution in higher PAHs. Several such entities are attempted to synthesize from viable starting materials. The ones realized experimentally are 1,2-BN naphthalene⁵⁴ 1,2-8,7-bis BN anthracenes, 9,10-BN phenanthrenes,⁵⁵ 4,5-9,10-bis BN pyrene and 1,5,9-Triaza-2,6,10-triphenlyboracoronene⁵⁶ etc. Position of the BN units in the carbocyclic rings

alters the properties of the systems largely. The 9,10-BN phenanthrene is observed to exhibit distinct photophysical properties with respect to the "internalized BN substituted phenanthrene."⁵⁷ Recently, in year 2014, Pie and co-workers have advent with double BN substituted coronene which shows a significant increase in the charge mobility. Lately, in year 2015, Pie and co-worker have further synthesized the three BN embedded coronene molecule as a model structure of BN-doped graphene and have asserted the opening in bandgap and modulation in electronic properties. Most recently, in year 2017, Dosso et al. has successfully synthesized⁵⁸ a coronene molecule which consists of "borazine-like inner" ring. However, the trend in the stability order of the corresponding isomers of these BN-substituted PAHs is not understood in details. Here, we have made a step forward in understanding the perturbation of the chemistry of coronene upon substitution with BN. We have studied the relative stability of the coronene entity by stepwise substitution of C-C bond with BN unit upto three steps. We start our investigation by computing the stability of the singly substituted BN-coronene and further extend to double and triple BN pair substitution. An analogy is built to understand the parameters, which define the stability and aromaticity of these systems. The substitution of a single C-C pairs with BN unit confirms that the positional isomer with adjacent B and N atoms are energetically more preferred. The effect of bond strength for the different bonds like C-N, C-B and N-B play a significant role in determining the stability trends of positional isomers. Whereas in the double and triple BN pair substituted isomers, charge separation also renders a support to rationalize the stability trends of positional isomers. The NICS_{zz}(1) values calculated at the approximate ring centers are used to characterize the aromatic nature of positional isomers acquired after BN substitution to coronene. The position of the BN units are found to tune the HOMO-LUMO gap of coronene. Thus these BN-substituted coronene molecules might show interesting opto-electronic properties.

[2.2] Computational Details

All the computations were carried out using Gaussian 09 package.²⁵ The structures were optimized at M06/cc-pvTZ level of theory.^{19,21} Harmonic vibrational frequencies were calculated to characterize the nature of stationary points. The reported structures attained energy minima on their corresponding potential energy

surfaces (PES). For the aromaticity evaluation, the $\text{NICS}_{\text{zz}}(1)^{34,35}$ has been calculated using the regular GIAO method at the centre of each of the rings ranging from 0.0 Å to 3.0 Å distances along the perpendicular axis to the molecular plane. NICS is defined as the negative value of the absolute shielding computed at a ring center or at some other interesting point of the system, for instance 1 Å above the ring center. Rings with large negative NICS values are considered aromatic. The more negative the NICS values, the more aromatic the rings are.

[2.3] Results and discussions

The Figure 1 shows the naming scheme used for representing the positional isomers obtained after substitution of the carbon atoms in coronene with B and N atoms. The carbon atoms in the outer ring are numbered from 1 to 18 whereas the inner ring atoms are numbered from 19 to 24. The isomers are denoted as n-aza,m-boracoronene, where n and m represents the carbon atoms which are substituted with boron and nitrogen atoms respectively. We start our investigation by analysing the possibilities of mono BN substituted coronene and further extend to double and triple BN pair substitution in step-wise manner.

[2.3.1] Mono BN pair substitution:

The substitution of single carbon atoms in the outer ring with B and N atoms give rise to total 31 positional isomers. When the position of the N atom is kept fixed at C1 (Fig. 1b) and the other carbon atoms in the outer ring are replaced with boron atoms, seventeen positional isomers are obtained. Another set of nine isomers are formed while keeping the N atom at one of the ring junctions of the outer ring, (i.e. C13, Fig 1b) and replacement of the other carbon atoms in the same ring with B atom. The Table A1 (Appendix) gives the relative energy (kcal/mol) difference of all the positional isomers obtained here. We found that the substitution of adjacent carbon atoms with boron and nitrogen atoms are more stable than those isomers where B and N atoms are far apart. In the similar way, the substitution of the carbon atoms in the inner ring would give few more positional isomers. But we restricted to

substitution of adjacent carbon atoms only. The relative energy values for these isomers are also given in Table A1 (**Appendix**). This is obvious that the adjacently placed B and N would provide the maximum stability due to the electrostatic charge separation between the B and N atoms. Unlike the C-C pair, the B-N pair is better understood as dipolar unit $B^{\delta-}-N^{\delta+}$, where the boron atom gets slight negative charges and N atom is slightly positive charged. Thus as the distance between this two opposite poles is increased the electrostatic interaction is decreased, leading to the decrease in stability of the isomers. However, the adjacent position of the B and N atoms do not provide equal stability to the positional isomers. The Figure (**2 I-V**) shows the five most stable isomers with their relative gibbs energy (kcal/mol) and the corresponding ring NICS_{zz}(1) values.

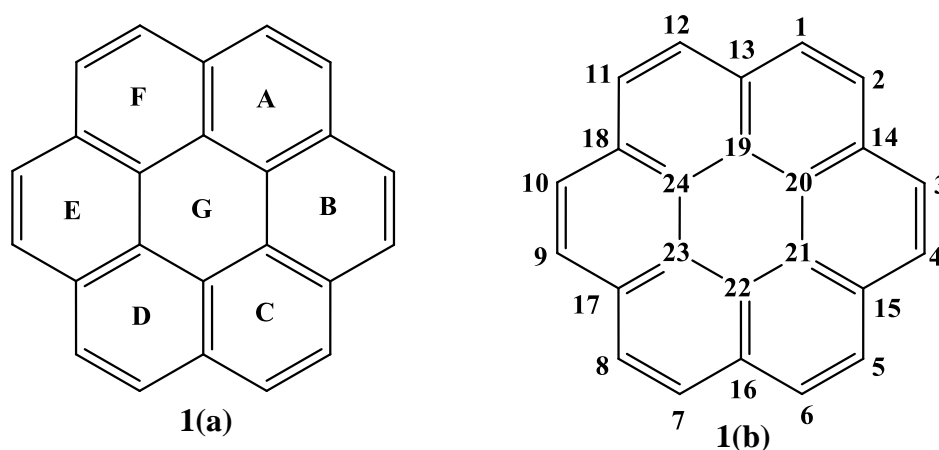


Figure 2.1(a) Schematic representation of Coronene where different rings are designated in capital alphabets from A to G; **1(b)** The numbering scheme of carbon atoms in the inner and outer rings of coronene.

The computations show that the isomer designated as 1-aza,2-boracoronene with boron and nitrogen atoms at terminal position in the outer ring is the most stable structure, whereas the isomer 19-aza,20-boracoronene with B and N atoms in the inner ring is less stable by 21.9 kcal/mol. The replacement of the carbon atoms in the ring junctions in both the inner and the outer rings also reduces the stability of the isomers. However, the boron atom substitution is slightly more favourable at the ring junction than the nitrogen atom. Thus the substitution of C13 (Figure **2-II**) with B and

N at C1 is the second most stable isomer. All the isomers with N placed at the ring junctions such as C13 or C19, are comparatively less stable w.r.t. the 1-aza,2-boracoronene and Figure 2-I), irrespective of the position of boron atom. The HOMO-LUMO separation of the five most stable positional isomers with mono BN substitution is also reported. Compared to unsubstituted coronene, the HOMO-LUMO differences increases for 2-III and 2-IV, whereas it decreases for the other three isomers. The aromaticity of the coronene ring undergo a significant change on substituting BN pairs to C=C bonds. The effect of the substitution on NICS_{zz}(1) is shown in Figure (2-1). The NICS_{zz}(1) of the ring containing the BN pair gets decreased w.r.t to unsubstituted coronene. Aromaticity of the rings gets reduced to a greater extent when N or B occupies ring junction position C19 as seen for isomer 2-III and 2-V. NICS_{zz}(1) value at the approximate center of the inner most ring becomes 7.14 ppm for 2-III, and for 2-IV, the value reduces to -1.40 ppm.

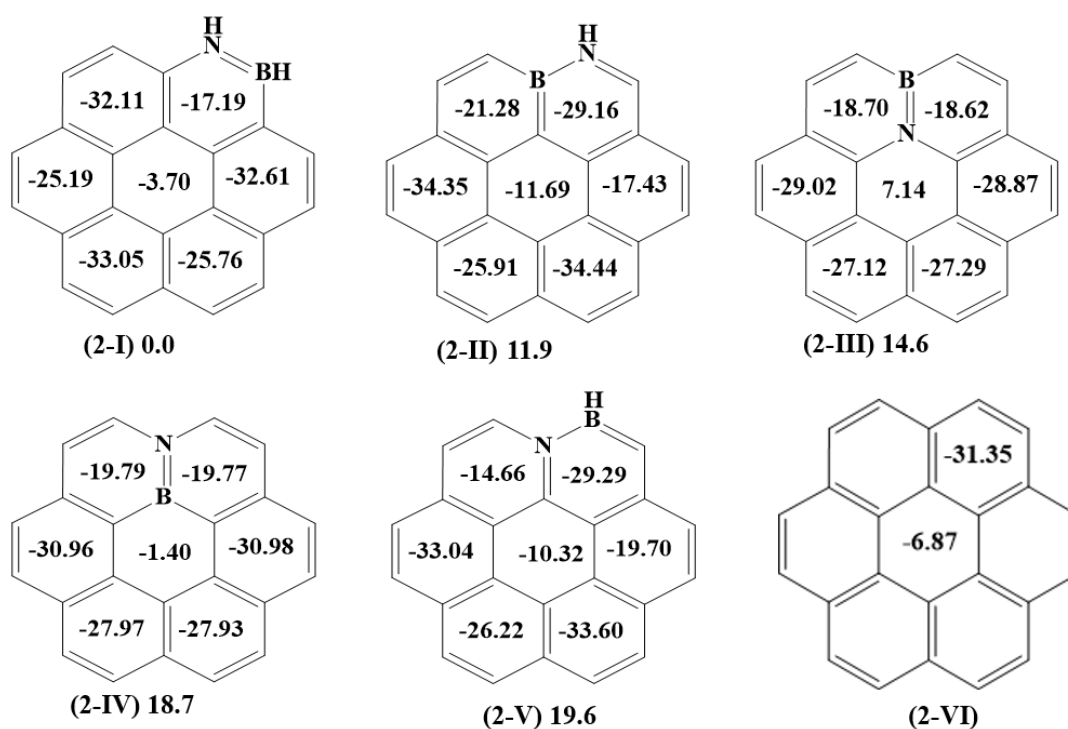


Figure 2.2 Schematic representation of five most stable mono BN pair substituted coronene with their relative gibbs energy at the bottom in kcal/mol. The number inside the ring represent the NICS_{zz}(1) values (in ppm) corresponding rings. **Figure**

(2-I)- 1-aza,2-boracoronene; **(2-II)** - 1-aza,13-boracoronene; **(2-III)** - 19-aza,13-boracoronene; **(2-IV)** - 13-aza,19-boracoronene; **(2-V)** - 13-aza,1-boracoronene; **(2-VI)** - unsubstituted coronene

In order to rationalize the relative stability of these positional isomers, the nbo charges on the carbon atoms of un-substituted coronene molecule (2-VI) is evaluated. The relative stability for the substitution of the carbon atoms by the heteroatoms with different electro-negativities could be understood by using Gimarc's rule.⁵⁸ According to this, an electronegative atom or group prefers to replace a site of higher electron density, whereas an electropositive atom prefers a site with low electron density. The Figure 3a shows the NBO charge distribution of unsubstituted coronene. The carbon atom at the terminal position carries the highest negative charge whereas at the ring junction it exhibits lower negative charges. Thus the isomer with N at the terminal position i.e. C1. and boron at the ring junction i.e C13 would be the most stable. This explains the instability of the isomers 2-III, 2-IV and 2-V, where the presence of N at the ring junction reduces the delocalization of the electron density of the rings and the NICS values at the hexagonal ring centres reduce. But the relative stability of 2-I vs 2-II could not be justified using the rule. Thus, the different bond strength values are considered to determine the relative stabilities of these two positional isomers. Table 1 shows the bond energy values for the different bonds and the number of different types of bonds in the five most stable isomers of mono-substituted BN coronene. On comparing the two most stable isomers, 1-aza,2-boracoronene and 1-aza,13-boracoronene, the major differences in the number of C-H vs B-H, C=C vs B=C, C-N vs B-N and C=N vs B=N bonds are found. The B-H bond in isomer 2-I is replaced by C-H group in isomer 2-II. This imparts a stabilization of 5.45 kcal to the isomer 2-II, whereas modification of C=C to B=C imparts a destabilization of around 1.54 kcal to this isomer. However, the stability of the C=N vs B=N compared to C-N vs B-N determines the relative stability.



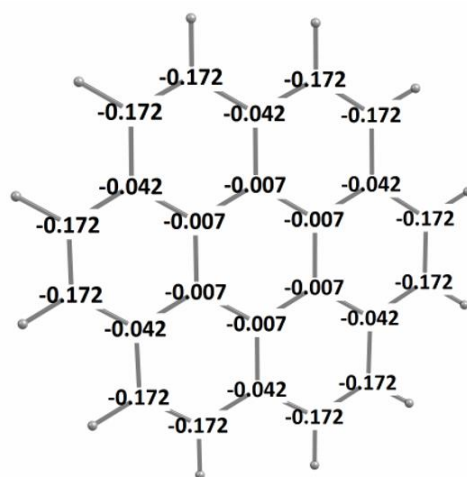
Here a near-isodesmic equation is shown to compare the stability of these bonds, sine relevant values for these bonds are not found in the literature. The stability of C=N is around twice as compared to C-N (Table 2.1). Despite, the ΔG for the reaction is exothermic by 19.34 kcal/mol.

This indicates that the relative stability of B=N vs B-N is much higher than the C=N vs C-N. Thus, though the replacement of C-N to C=N in isomer 2-II would enhance its stability, the presence of B-N bond compared to B=N in isomer 2-I reduces its overall stability.

Table 2.1: The relative energy (kcal/mol), HOMO-LUMO gap (kcal/mol) and different types of bonds present in the five most isomers of single BN substituted coronene. The HOMO-LUMO gap for coronene is 101.3 kcal/mol. The bond energy values are taken from standard Inorganic text book.⁵⁹

<i>isomers</i>		2-I	2-II	2-III	2-IV	2-V
R.E. (kcal/mol)		0.0	11.9	14.6	18.7	19.6
HUMO-LUMO gap (kcal/mol)		92.5	79.8	99.3	100.7	79.6
<i>Bond Types</i>	Bond Energy (kcal/mol)	<i>No. of Bond types present in isomers</i>				
C-H	98.3	10	11	12	12	11
B-H	93	1	0	0	0	1
N-H	92	1	1	0	0	0
B-N	-	0	1	0	0	1
B=N	-	1	0	1	1	0
C-C	82.6	16	16	14	14	16
C=C	144	11	10	11	11	10
B-C	89.0	1	1	2	2	0
B=C	*	0	1	0	0	1
N-C	72.8	1	0	2	2	1
N=C	147	0	1	0	0	1

* See Appendix A4:



(a)

Figure 2.3: The calculated NBO charges for Coronene.

[2.3.2] Double pair BN substitution:

The structures and the stability of positional isomers obtained from double BN pairs substitution to coronene is investigated. The relative gibbs energies (kcal/mol) of five most stable isomers with respect to the minimum energy structure is reported in Figure 2.4 and remaining ones are provided in Table A2 (Appendix). The most stable isomers of mono-BN substituted coronene is taken to substitute the different C-C bonds with BN consecutively in the inner and the outer rings of coronene to obtain the double BN pair substituted coronene. This provides total twenty-four positional isomers.

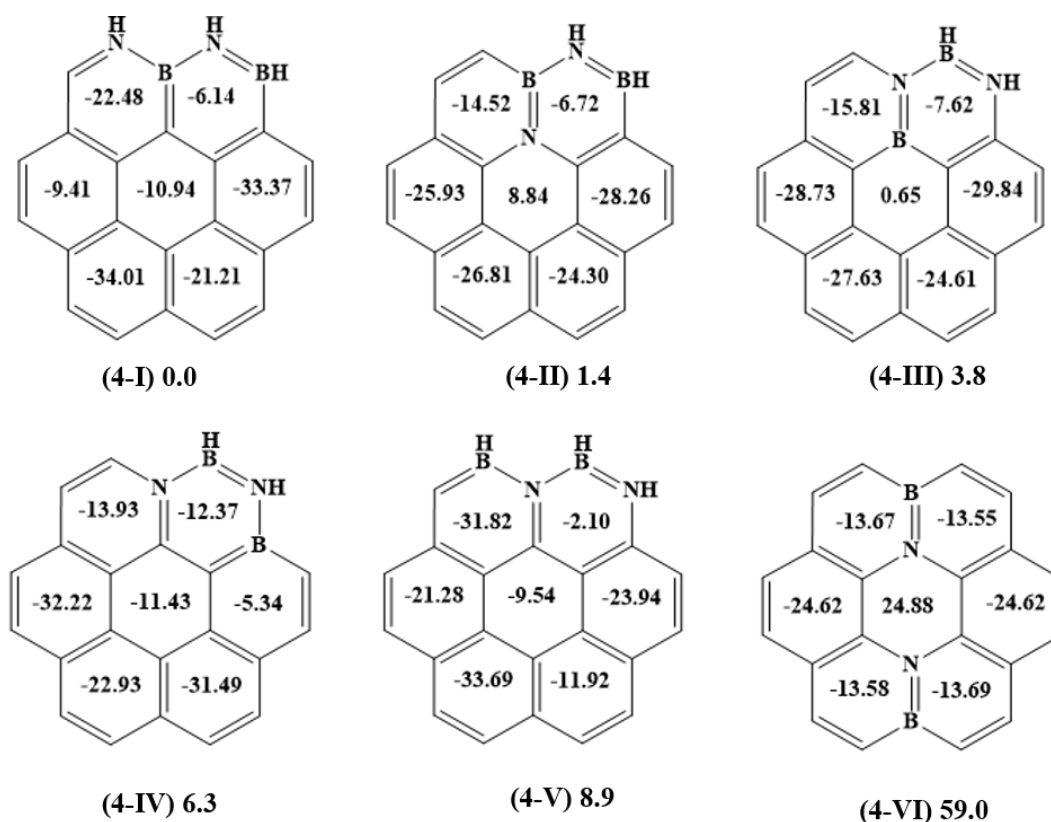
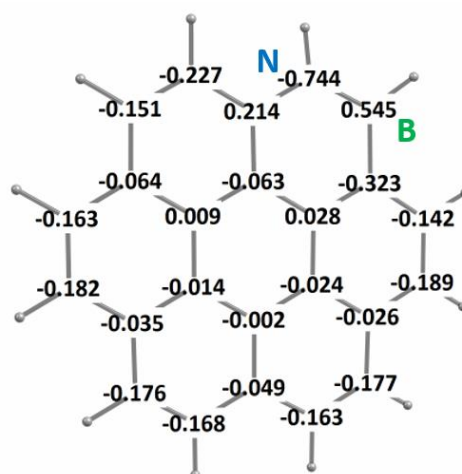


Figure 2.4 Schematic representation of five most stable double BN pair substituted coronene with their relative gibbs energy at the bottom in kcal/mol. The number inside the ring represent the NICS_{zz}(1) values (in ppm) corresponding rings. **Figure**

(4-I) - 1,12-aza,2,13-boracoronene; **(4-II)** - 1,19-aza,2,13-boracoronene; **(4-III)** - 2,13-aza,1,19-boracoronene; **(4-IV)** - 2,13-aza,1,14-boracoronene; **(4-V)** - 2,13-aza,1,12-boracoronene; **(4-VI)** – 19,22-aza,13,16-boracoronene

Among all the isomers the most stable positional isomer, 1,12-aza,2,13-boracoronene (Figure 4-I), consists of adjacent BN pairs with two nitrogen and one boron at terminal position and the other boron at ring junction. The movement of one of the nitrogen atoms from terminal position i.e, C12 to the inner ring i.e. C19 (isomer 1,19-aza,2,13-boracoronene, Figure 4-II) stability reduces by 1.4 kcal/mol. The stability is also reduced by interchanging the positions of B and N atoms in isomers 4-I and 4-II, giving rise to isomers 4-III and 4-V. The isomer (4-IV) obtained after shifting one of the boron atoms in the isomer 4-I from C13 to C14 (the ring junction) the stability is reduced by 6.3 kcal/mol. Figure 4-VI represents the experimentally synthesized di-BN substituted coronene which is less stable by 59.0 kcal w.r.t the most stable isomer 4-I. It is due to the non-adjacent position of the BN pairs. The HOMO-LUMO gap for the five most stable isomers varies within the range of 77.7 to 95.3 kcal/mol. The experimental isomer 3-VI has the HOMO-LUMO separation of around 98.3 kcal/mol. Thus the position of the BN pairs would enable to tune the HOMO-LUMO separation of the molecule, without affecting the stability of the system to a greater extent. The Figure 4 shows the NICSzz(1) values for the most stable five double BN pair substituted isomers. In these cases, the aromaticity of the rings containing the BN pairs reduces. The NICSzz(1) values for the inner hexagonal ring becomes antiaromatic for the isomers 3-II and 3-III. Whereas for the other three isomers, the aromaticity of the inner ring increases w.r.t the most stable mono-substituted BN isomer (2-I).



29

(a)

Figure 2.5: The calculated NBO charges for 1-aza,2-boracoronene (**2-I**).

The charge distribution analysis of the most stable mono-BN pair substituted coronene (**2-I**) shown in Figure **2.5**, reveals the relative stability order of the di-substituted BN coronene isomers. The carbon atom C13, placed next to the nitrogen atom has the highest partial positive charges suitable for the position of boron atoms whereas two carbon atoms C12 and C14 has the highest negative charges suitable for the nitrogen atom. This give rise to the two possibilities isomers **4-I** and **4-IV**. However, the relative stability of the previous one is greater, due to the involved bond strengths of the different types of bonds present in the two isomers. In the previous isomer one N-H bond is converted to C-H bond, favouring the latter structure by 6.3 kcal. But the replacement of C-C bond to N-C destabilizes the latter structure by 9.8 kcal. In addition, the number of B=N vs B-N bonds are also responsible for reducing the relative stability of the isomer 4-IV. In the isomer 4-IV, one B=N and two B-N bonds are present, whereas the isomer 4-I has one B-N and two B=N bonds.

Table 2.2: The relative energy (kcal/mol), HOMO-LUMO gap (kcal/mol) and different types of bonds present in the five most isomers of double BN substituted coronene. The HOMO-LUMO gap for experimentally known di-BN substituted coronene is 98.3 kcal/mol. The bond energy values are taken from standard Inorganic text book.⁵⁹

<i>isomers</i>	4-I	4-II	4-III	4-IV	4-V		
R.E. (kcal/mol)	0.0	1.4	3.8	6.3	8.9		
HOMO-LUMO gap (kcal/mol)	77.7	94.6	95.3	79.3	78.0		
<i>Bond Types</i>	Bond Energy (kcal/mol)		<i>No. of Bond types present in isomers</i>				
C-H	98.3	9	10	10	10	9	
B-H	93	1	1	1	1	2	
N-H	92	2	1	1	1	1	
B-N	-	1	1	1	2	2	
B=N	-	2	2	2	1	1	
C-C	82.6	15	13	13	14	15	
C=C	144	9	10	10	9	9	
B-C	89.0	1	2	2	1	0	
B=C	*	1	0	0	1	1	
N-C	72.8	0	2	2	1	1	
N=C	147	1	0	0	1	1	

* See Appendix A4

[2.3.3] Triple pair BN substitution:

The positional isomers of triple BN pairs substitution is derived by addition of another BN pair in different positions of the inner and outer ring of the most stable double BN pair substituted structures. In this way 37 unique positional isomers are found, out of which the five most stable isomers are shown in Figure. 2.6. The relative stabilities of all the positional isomers are given in Table A3 (Appendix). The global minimum isomer, 1,14,19-aza,2,13,20-boracoronene (**6-I**), comprises of a borazine-like ring in the outer ring of the coronene molecule. However, when a similar arrangement of the BN pairs are made in the inner ring as isomer **6-V**, the stability is reduced by 23.8 kcal/mol. The second most stable structure is 2,3,13-aza,1,4,14-boracoronene (**6-II**), obtained from 4-IV, by substituting the terminal C-C unit in the next ring. Other two isomers **6-III** and **6-V** are obtained when the most stable double BN substituted isomer is provided with another BN unit in the inner and the outer ring respectively. For both the isomers the relative stabilities are less than **6-I**. The structure **6-VI** represents the experimentally reported structure with three BN pairs by Wang et al. which is 15.7 kcal higher in energy w.r.t the most stable structure **6-I**. In the triply BN substituted coronene isomers, **6-VI** has the highest value for HOMO-LUMO gap of around 108.5 kcal/mol. The most stable isomers **6-I** shows a gap of around 94.5 kcal/mol, slightly less than that of the experimental structure. For the other isomers, the gap varies from 70.6 to 94.5 kcal/mol. As an indicator of the aromaticity, the NICS_{zz}(1) values shows a similar trend as seen for the single and double BN substituted isomers. The values are found to be less for the rings containing the BN pairs in comparison to those rings without any BN pairs. The NICS_{zz}(1) values for the inner rings shows aromaticity for the isomers **6-II**, **6-IV** and **6-V**. In other cases, the NICS_{zz}(1) values are either positive (isomer **6-I**) or negative with very less magnitudes (isomer **6-III** and **6-VI**).

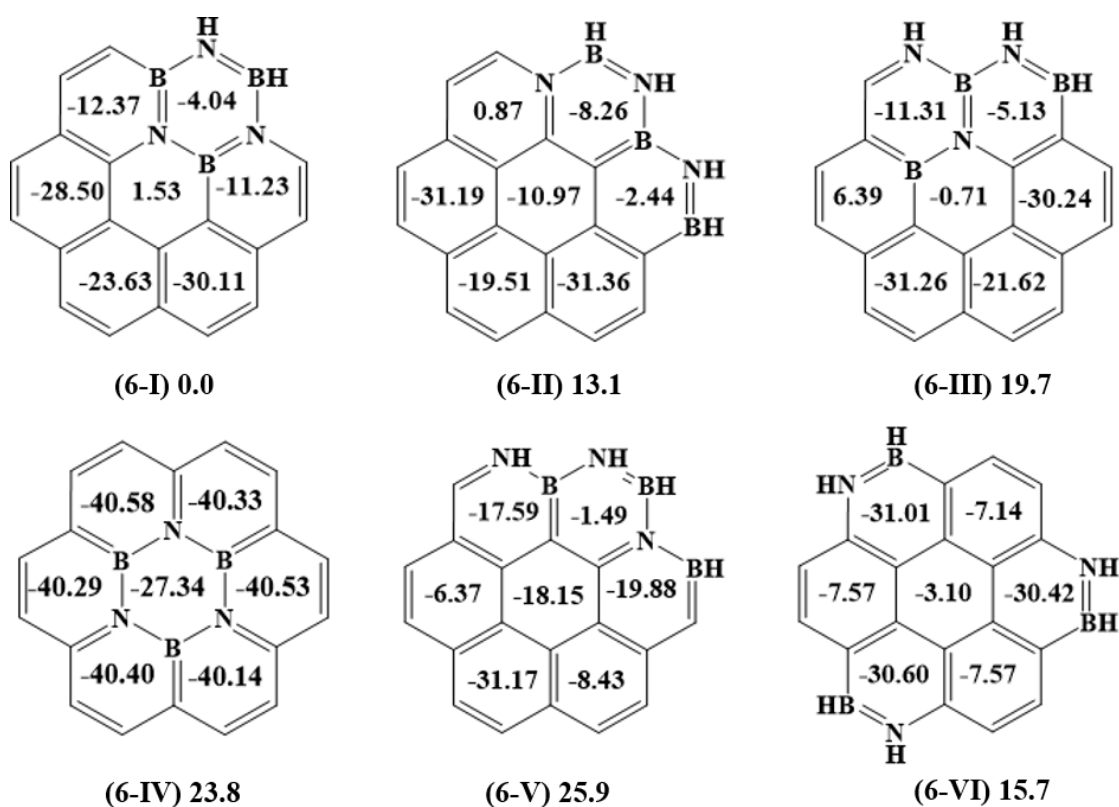


Figure 2.6 Schematic representation of five most stable triple BN pair substituted coronene with their relative gibbs energy at the bottom in kcal/mol. The number inside the ring represent the NICS_{zz}(1) values (in ppm) corresponding rings. **Figure (6-I)** - 1,14,19-aza,2,13,20-boracoronene; **(6-II)** - 2,3,13-aza,1,4,14-boracoronene; **(6-III)** - 1,12,19-aza,2,13,24-boracoronene; **(6-IV)** - 19,21,23-aza,20,22,24-boracoronene; **(6-V)** - 1,12,14-aza,2,3,13-boracoronene; **(6-VI)** - 3,7,11-aza,4,8,12-boracoronene

In order to rationalize the relative stability, the NBO charges of the most stable doubly substituted BN isomer is evaluated and shown in Figure 2.7. The charge distribution exhibits that C20 and C14 position carry the highest partial positive and negative charges respectively. This observation provides us an idea that C14 and C20 position is the most suitable place for boron and nitrogen atom substitution. The corresponding substitution leads to the global minimum structure with borazine ring in the outer ring of the coronene designated as the **6-I** isomer. The bond energy values shown in Table 2.3 further justify the stability ordering of the isomers. The isomer **6-I** has the maximum number of C-H and B=N bonds compared to other isomers, which imparts a higher stability to this isomer compared to the other isomers.

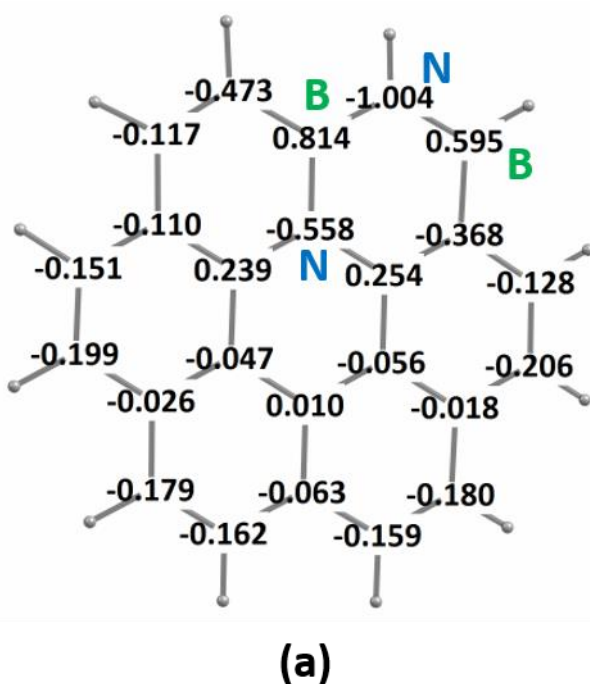


Figure 2.7: The calculated NBO charges for (**4-I**).

Table 2.3: The relative energy (kcal/mol), HOMO-LUMO gap (kcal/mol) and different types of bonds present in the five most isomers of triple BN substituted coronene. The HOMO-LUMO gap for experimentally known tri-BN substituted coronene is 108.5 kcal/mol. The bond energy values are taken from standard Inorganic text book.⁵⁹

<i>isomers</i>	6-I	6-II	6-III	6-IV	6-V	
R.E. (kcal/mol)	0.0	13.1	19.7	23.8	25.9	
HUMO-LUMO gap (kcal/mol)	94.5	81.0	87.4	82.8	70.6	
<i>Bond Types</i>	Bond Energy (kcal/mol)	<i>No. of Bond types present in isomers</i>				
C-H	98.3	10	8	9	12	8
B-H	93	1	2	1	0	2
N-H	92	1	2	2	0	2
B-N	-	0	1	1	3	2
B=N	-	3	2	2	0	1
C-C	82.6	11	13	14	12	14
C=C	144	9	8	8	6	7
B-C	89.0	1	1	1	0	0
B=C	*	1	1	1	3	2
N-C	72.8	1	1	1	0	0
N=C	147	1	1	1	3	2

* See Appendix A4

[2.4] Conclusion

The effect of single, double and triple BN pairs substitution on coronene molecule is studied. The most stable single BN pair substituted corresponds to the structure with B and N atoms present at the terminal position of the outer ring in coronene (1-aza,2-boracoronene). The stability of the positional isomers reduces as the substitution is made in the inner ring. In case of double BN substitution, the most stable positional isomer consists of two adjacently placed BN pairs among which the N atoms and one B atom are placed at the terminal position whereas another B atom at the ring junction (1,12-aza,2,13-boracoronene). The boron atom prefers to be at ring junction and nitrogen atom at the terminal position of the outer ring. Stability of the positional isomers decrease when substitution is done inside the inner ring. The most stable positional isomer for triple BN substituted coronene system contains borazine-like ring in the outer ring. The charge separation and the different bond strength like C-B, N-C, B-N play the crucial role to determine the relative stabilities of different positional isomers. Substitution of the C-C bond with BN pair decreases the aromaticity of all the outer rings as seen from the calculated the NICS_{zz}(1) values at

the approximate ring centers of the six membered rings. However, for the inner hexagonal ring the NICS_{zz}(1) values do not show a simple trend. The values varies from the negative magnitudes to positive ones. The HOMO-LUMO gap also shows great variations in their magnitudes depending upon the position of the B and N atoms in the rings. In comparison to the experimental structures, the isomers reported in this study are more stable and have reasonable separations of the HOMO and LUMO orbitals. Thus these molecules might behave as suitable materials with superior opto-electronic properties.

[2.5] Future Direction

In our present report, the investigation is made up to triple BN pair substitution which need to be further extended for four BN units replacement. There is no idea about the relation of aromaticity and stability is obtained from NICS(1)_{zz} calculations, hence, the aromaticity assessment using electronic based aromatic indices is to be evaluated.

[2.5] References

1. Schleyer, P. v. R.; Jiao, (a) Schleyer, P. v. R.; Jiao, H., What is aromaticity? *Pure Appl. Chem.* **1996**, *68* (2), 209-218
2. Hückel, E., Quantentheoretische Beiträge zum Benzolproblem I. Die Elektronenkonfiguration des Benzols und verwandter Verbindungen. *Z. Physik* **1931**, *70*, 104-186
3. Clar, E., *The Aromatic Sextet*. Wiley: New York, 1972; (b) Solà, M., Forty years of Clar's aromatic π -sextet rule. *Front Chem* **2013**, *1*, 22.
4. Glidewell, C.; Lloyd, D., MNDO study of bond orders in some conjugated bi- and tri-cyclic hydrocarbons. *Tetrahedron* **1984**, *40*, 4455-4472.
5. El Bakouri, O.; Poater, J.; Feixas, F.; Solà, M., Exploring the validity of the Glidewell–Lloyd extension of Clar's π -sextet rule: assessment from polycyclic conjugated hydrocarbons. *Theor. Chem. Acc.* **2016**, *135* (8), 205.

6. Portella, G.; Poater, J.; Solà, M., Assessment of the Clar's aromatic pi-sextet rule by means of PDI, NICS, and HOMA indicators of local aromaticity. *J. Phys. Org. Chem.* **2005**, *18*, 785-791
7. Zubarev, D. Y.; Boldyrev, A. I., Developing paradigms of chemical bonding: adaptive natural density partitioning. *Phys. Chem. Chem. Phys.* **2008**, *10* (34), 5207-5217.
8. Foster, J. P.; Weinhold, F., Natural Hybrid Orbitals. *J. Am. Chem. Soc.* **1980**, *102*, 7211-7218; (b) Reed, A. E.; Curtiss, L. A.; Weinhold, F., Intermolecular interactions from a natural bond orbital, donor-acceptor viewpoint. *Chem. Rev.* **1988**, *88* (6), 899-926.
9. Sergeeva, A. P.; Zubarev, D. Y.; Zhai, H.-J.; Boldyrev, A. I.; Wang, L.-S., A Photoelectron Spectroscopic and Theoretical Study of B16⁻ and B162⁻: An All-Boron Naphthalene. *J. Am. Chem. Soc.* **2008**, *130* (23), 7244-7246
10. Zubarev, D. Y.; Boldyrev, A. I., Revealing Intuitively Assessable Chemical Bonding Patterns in Organic Aromatic Molecules via Adaptive Natural Density Partitioning. *J. Org. Chem.* **2008**, *73* (23), 9251-9258
11. Watson, M. D.; Jäckel, F.; Severin, N.; Rabe, J. P.; Müllen, K., A Hexa-peri-hexabenzocoronene Cyclophane: An Addition to the Toolbox for Molecular Electronics. *J. Am. Chem. Soc.* **2004**, *126* (5), 1402-1407
12. Kmak, W. S.; Yatabe, A. Method for removing coronene from heat exchangers. US4222852 A, 1980.
13. Clar, E.; Sanigök, Ü.; Zander, M., NMR studies of perylene and coronene derivatives. *Tetrahedron* **1968**, *24* (7), 2817-2823.
14. Aihara, J.-i., The origin of counter-rotating rim and hub currents in coronene. *Chem. Phys. Lett.* **2004**, *393* (1-3), 7-11
15. Huang, W.; Sergeeva, A. P.; Zhai, H.-J.; Averkiev, B. B.; Wang, L.-S.; Boldyrev, A. I., A concentric planar doubly π -aromatic B19⁻ cluster. *Nat. Chem.* **2010**, *2* (3), 202-206.
16. Jiménez-Halla, J. O. C.; Islas, R.; Heine, T.; Merino, G., B19⁻: An Aromatic Wankel Motor. *Angew. Chem. Int. Ed. (English)* **2010**, *49* (33), 5668-5671.
17. Kutzelnigg, W., What I like about Hückel theory. *J. Comput. Chem.* **2007**, *28* (1), 25-34.

18. Dewar, M. J. S., Chemical implications of s conjugation. *J. Am. Chem. Soc* **1984**, *106* (3), 669-682.
19. Zhao, Y.; Truhlar, D. G., The M06 suite of density functionals for main group thermochemistry, thermochemical kinetics, noncovalent interactions, excited states, and transition elements: two new functionals and systematic testing of four M06-class functionals and 12 other functionals. *Theor. Chem. Acc.* **2008**, *120* (1), 215-241.
20. Becke, A. D., Density-functional thermochemistry. III. The role of exact exchange. *J. Chem. Phys.* **1993**, *98* (7), 5648-5652;
21. Dunning Jr., T. H., Gaussian basis sets for use in correlated molecular calculations. I. The atoms boron through neon and hydrogen. *J. Chem. Phys.* **1989**, *90* (2), 1007-1023.
22. Grimme, S.; Antony, J.; Ehrlich, S.; Krieg, H., A consistent and accurate ab initio parametrization of density functional dispersion correction (DFT-D) for the 94 elements H-Pu. *J. Chem. Phys.* **2010**, *132* (15), 154104.
23. Becke, A. D.; Johnson, E. R., A density-functional model of the dispersion interaction. *J. Chem. Phys* **2005**, *123* (15), 154101
24. Karton, A., How reliable is DFT in predicting relative energies of polycyclic aromatic hydrocarbon isomers? comparison of functionals from different rungs of jacob's ladder. *J. Comput. Chem* **2016**, ASAP.
25. Frisch, M. J.; Trucks, G. W.; Schlegel, H. B.; Scuseria, G. E.; Robb, M. A.; Cheeseman, J. R.; Scalmani, G.; Barone, V.; Mennucci, B.; Petersson, G. A.; Nakatsuji, H.; Caricato, M.; Li, X.; Hratchian, H. P.; Izmaylov, A. F.; Bloino, J.; Zheng, G.; Sonnenberg, J. L.; Hada, M.; Ehara, M.; Toyota, K.; Fukuda, R.; Hasegawa, J.; Ishida, M.; Nakajima, T.; Honda, Y.; Kitao, O.; Nakai, H.; Vreven, T.; Montgomery, J., J. A.; Peralta, J. E.; Ogliaro, F.; Bearpark, M.; Heyd, J. J.; Brothers, E.; Kudin, K. N.; Staroverov, V. N.; Kobayashi, R.; Normand, J.; Raghavachari, K.; Rendell, A.; Burant, J. C.; Iyengar, S. S.; Tomasi, J.; Cossi, M.; Rega, N.; Millam, J. M.; Klene, M.; Knox, J. E.; Cross, J. B.; Bakken, V.; Adamo, C.; Jaramillo, J.; Gomperts, R.; Stratmann, R. E.; Yazyev, O.; Austin, A. J.; Cammi, R.; Pomelli, C.; Ochterski, J. W.; Martin, R. L.; Morokuma, K.; Zakrzewski, V. G.; Voth, G. A.; Salvador, P.; Dannenberg, J. J.; Dapprich, S.; Daniels, A. D.; Farkas, Ö.; Foresman, J. B.; Ortiz, J.

V.; Cioslowski, J.; Fox, D. J. *Gaussian 09, Revision C.01*, Gaussian, Inc.: Wallingford CT, 2009.

26. A Critical Assessment of the Performance of Magnetic and Electronic Indices of Aromaticity. *Symmetry* **2010**, *2*, 1156-1179.

27. Krygowski, T. M.; Szatyłowicz, H.; Stasyuk, O. A.; Dominikowska, J.; Palusiak, M., Aromaticity from the Viewpoint of Molecular Geometry: Application to Planar Systems. *Chem. Rev.* **2014**, *114* (12), 6383-6422.

28. Kruszewski, J.; Krygowski, T. M., Definition of aromaticity basing on the harmonic oscillator model. *Tetrahedron Lett.* **1972**, *13* (36), 3839-3842

29. Feixas, F.; Matito, E.; Poater, J.; Solà, M., Quantifying aromaticity with electron delocalisation measures. *Chem. Soc. Rev.* **2015**, *44*, 6434–6451

30. Poater, J.; Fradera, X.; Duran, M.; Solà, M., The Delocalization Index as an Electronic Aromaticity Criterion. Application to a Series of Planar Polycyclic Aromatic Hydrocarbons. *Chem. Eur. J.* **2003**, *9*, 400-406.

31. Matito, E.; Duran, M.; Solà, M., The aromatic fluctuation index (FLU): A new aromaticity index based on electron delocalization. *J. Chem. Phys.* **2005**, *122* (1), 014109.

32. Giambiagi, M.; de Giambiagi, M. S.; dos Santos Silva, C. D.; de Figueiredo, A. P., Multicenter bond indices as a measure of aromaticity. *Phys. Chem. Chem. Phys.* **2000**, *2* (15), 3381-3392.

33. Mitchell, R. H., Measuring aromaticity by NMR. *Chem. Rev.* **2001**, *101* (5), 1301-1315

34. Schleyer, P. v. R.; Maerker, C.; Dransfeld, A.; Jiao, H.; van Eikema Hommes, N. J. R., Nucleus-Independent Chemical Shifts: A simple and Efficient Aromaticity Probe. *J. Am. Chem. Soc.* **1996**, *118*, 6317-6318

35. Wolinski, K.; Hilton, J. F.; Pulay, P., Efficient Implementation of the Gauge-Independent Atomic Orbital Method for NMR Chemical Shift Calculations. *J. Am. Chem. Soc.* **1990**, *112*, 8251-8260.

36. Gershoni-Poranne, R.; Stanger, A., The NICS-XY-Scan: Identification of Local and Global Ring Currents in Multi-Ring Systems. *Chem. Eur. J.* **2014**, *20* (19), 5673-5688.

37. Matito, E. *ESI-3D: Electron Sharing Indexes Program for 3D Molecular Space Partitioning*. <http://iqc.udg.es/~eduard/ESI>, Institute of Computational Chemistry and Catalysis: Girona, **2006**.
38. Keith, A. *AIMall* (v. 14.11.23), TK Gristmill Software (aim.tkgristmill.com): Overland Park KS, USA, 2014.
39. Bader, R. F. W., *Atoms in Molecules: A Quantum Theory*. Clarendon: Oxford, **1990**
- 40(a). Brock, C. P.; Dunitz, J. D.: Temperature dependence of thermal motion in crystalline naphthalene. *Acta Crystallogr.* **1982**, B38, 2218-2228.
- 40(b). Kay, M. I.; Okaya, Y.; Cox, D. E., A refinement of the structure of the room-temperature phase of phenanthrene, C₁₄H₁₀, from X-ray and neutron diffraction data. *Acta Crystallogr., Sect. B* **1971**, 27 (1), 26-33.
41. Camerman, A.; Trotter, J.: The crystal and molecular structure of pyrene. *Acta Crystallogr.* **1965**, 18, 636-643
42. Krygowski, T. M.; Cyrański, M.; Ciesielski, A.; Świrski, B.; Leszczyński, P., Separation of the Energetic and Geometric Contributions to Aromaticity. 2. Analysis of the Aromatic Character of Benzene Rings in Their Various Topological Environments in the Benzenoid Hydrocarbons. Crystal and Molecular Structure of Coronene. *J. Chem. Inf. Model.* **1996**, 36 (6), 1135-1141.
43. Osuna, S.; Poater, J.; Bofill, J. M.; Alemany, P.; Solà, M., Are nucleus-independent (NICS) and ¹N NMR chemical shifts good indicators of aromaticity in *p*-stacked polyfluorenes? *Chem. Phys. Lett.* **2006**, 428, 191-195
44. Schulman, J. M.; Disch, R. L., Thermal and Magnetic Properties of Coronene and Related Molecules. *J. Phys. Chem. A* **1997**, 101 (48), 9176-9179.
45. Berionni, G.; Wu, J. I. C.; Schleyer, P. v. R., Aromaticity Evaluations of Planar [6]Radialenes. *Org. Lett.* **2014**, 16 (23), 6116-6119.
46. Matito, E.; Feixas, F.; Solà, M., Electron delocalization and aromaticity measures within the Hückel molecular orbital method. *J MOL STRUC-THEOCHEM* **2007**, 811 (1–3), 3-11.
47. Vijayalakshmi, K. P.; Suresh, C. H., Pictorial representation and validation of Clar's aromatic sextet theory using molecular electrostatic potentials. *New J. Chem.* **2010**, 34 (10), 2132-2138.

48. Dappe, Y. J.; Andersen, M.; Balog, R.; Hornekær, L.; Bouju, X., Adsorption and STM imaging of polycyclic aromatic hydrocarbons on graphene. *Phys Rev B* **2015**, *91* (4), 045427.
49. Aihara, J.-i., Nucleus-independent chemical shifts and local aromaticities in large polycyclic aromatic hydrocarbons. *Chem. Phys. Lett.* **2002**, *365* (1-2), 34-39
50. Rao, C. N. R.; Matte, H. S. S. R.; Subrahmanyam, K. S., Synthesis and Selected Properties of Graphene and Graphene Mimics. *Acc. Chem. Res* **2013**, *46* (1), 149-159.
51. Ci, L.; Song, L.; Jin, C.; Jariwala, D.; Wu, D.; Li, Y.; Srivastava, A.; Wang, Z. F.; Storr, K.; Balicas, L.; Liu, F.; Ajayan, P. M., Atomic layers of hybridized boron nitride and graphene domains. *Nat Mater* **2010**, *9* (5), 430-435.
52. Fang, X.; Yang, H.; Kampf, J. W.; Banaszak Holl, M. M.; Ashe, A. J., Syntheses of Ring-Fused B-N Heteroaromatic Compounds. *Organometallics* **2006**, *25* (2), 513-518.
53. Marwitz, A. J. V.; Matus, M. H.; Zakharov, L. N.; Dixon, D. A.; Liu, S.-Y., A Hybrid Organic/Inorganic Benzene. *Angew. Chem. Int. Ed. (English)* **2009**, *48* (5), 973-977.
54. Dewar, M. J. S.; Dietz, R. O. Y., New Heteroaromatic Compounds. XV.1 Halogenation of 2-Methyl-2,1-borazaronaphthalene. *J. Org. Chem* **1961**, *26* (9), 3253-3256
55. Dewar, M. J. S.; Kubba, V. P.; Pettit, R., 624. New heteroaromatic compounds. Part I. 9-Aza-10-boraphenanthrene. *J. Chem Soc (Resumed)* **1958**, (0), 3073-3076.
56. Li, G.; Xiong, W.-W.; Gu, P.-Y.; Cao, J.; Zhu, J.; Ganguly, R.; Li, Y.; Grimdale, A. C.; Zhang, Q., 1,5,9-Triaza-2,6,10-triphenylboracoronene: BN-Embedded Analogue of Coronene. *Org. Lett.* **2015**, *17* (3), 560-563.
57. Bosdet, M. J. D.; Piers, W. E.; Sorensen, T. S.; Parvez, M., 10a-Aza-10b-borapyrenes: Heterocyclic Analogues of Pyrene with Internalized BN Moieties. *Angew. Chem. Int. Ed. (English)* **2007**, *46* (26), 4940-4943.
58. Dosso, J.; Tasseroul, J.; Fasano, F.; Marinelli, D.; Biot, N.; Fermi, A.; Bonifazi, D.: Synthesis and Optoelectronic Properties of Hexa-peri-hexabenzoborazinocoronene *Angew. Chem. Int. Ed. (English)* **2017**, *56*, 4483-4487.

59. Ott, J. J.; Gimarc, B. M., Predictions of relative stabilities among series of carborane isomers by the criterion of topological charge stabilization. *J. Am. Chem. Soc.* **1986**, *108* (15), 4303-4308.
60. Huheey, J. E.; Keiter, E. A.; Keiter, R. L.; Medhi, O. K., *Inorganic chemistry: principles of structure and reactivity*. Pearson Education India: 2006.

Supporting Information

Table S1. B3LYP-D3(BJ)/cc-pVTZ values of reaction energies and energy barriers for the investigated PAHs. Enthalpies and Gibbs energies in kcal mol⁻¹.

Compound	Bonds ^a	ΔH_r	ΔG_r	ΔH^\ddagger	ΔG^\ddagger
Naphthalene exo	C1–C2	9.61	23.76	33.86	39.78
Phenanthrene exo	C9–C10	5.10	19.70	31.36	37.22
Pyrene exo	C9–C10	4.90	18.60	31.13	36.53
Coronene exo	C3–C4	9.59	22.59	33.82	38.95
Naphthalene endo	C1–C2	9.75	23.90	34.64	39.65
Phenanthrene endo	C9–C10	5.38	19.22	31.98	36.87
Pyrene endo	C9–C10	4.49	18.12	32.84	37.10
Coronene endo	C3–C4	9.27	22.09	37.33	41.18

Table S2. M06-2X/cc-pVTZ values of reaction energies and energy barriers for the investigated PAHs. Enthalpies and Gibbs energies in kcal mol⁻¹.

Compound	Bonds ^a	ΔH_r	ΔG_r	ΔH^\ddagger	ΔG^\ddagger
Naphthalene endo	C1–C2	1.09	14.65	31.24	35.70
Phenanthrene endo	C9–C10	-4.32	9.48	28.52	32.48
Pyrene endo	C9–C10	-5.25	8.37	28.33	32.49
Coronene endo	C3–C4	-0.12	12.51	33.82	36.80
Pyrene exo	C9–C10	-4.69	8.96	27.71	33.03

Table S3. B3LYP-D3(BJ)/cc-pVTZ and M06-2x/cc-pVTZ values of PDI, MCI, and I_{ring} (in electrons), FLU, HOMA, and NICS (in ppm) for the pyrene molecule (see Figure 1.2 for ring labels).

Indices	Ring	B3LYP-D3(BJ)/cc-pVTZ	M06-2X/cc-pVTZ
PDI	A	0.070	0.072
FLU	B	0.044	0.043
	A	0.007	0.006
MCI	B	0.020	0.021
	A	0.035	0.037
I_{ring}	B	0.018	0.017
	A	0.026	0.026
HOMA	B	0.014	0.014
	A	0.886	0.886
NICS(1) _{zz}	B	0.629	0.629
	A	-36.23	-37.46
	B	-16.88	-18.42

Appendix

Table A1: Relative gibbs energies of the positional isomers obtained by the substitution of two carbon atoms with boron and nitrogen atoms.

Positional Isomers	Relative Energy (kcal/mol)
1-aza,2-boracoronene	0.00
1-aza,13-boracoronene	11.87
19-aza,13-boracoronene	14.63
13-aza,19-boracoronene	18.70
13-aza,1-boracoronene	19.55
19-aza,20-boracoronene	21.92
1-aza,14-boracoronene	37.03
1-aza,11-boracoronene	40.16
13-aza,14-boracoronene	40.77
1-aza,3-boracoronene	41.31
1-aza,15-boracoronene	41.44
1-aza,12-boracoronene	43.59
13-aza,2-boracoronene	45.42
1-aza,6-boracoronene	46.08
1-aza,18-	47.19

boracoronene	
1-aza,5-boracoronene	47.62
1-aza,17-boracoronene	48.93
13-aza,4-boracoronene	49.50
1-aza,10-boracoronene	50.44
1-aza,16-boracoronene	51.93
1-aza,9-boracoronene	52.55
1-aza,5-boracoronene	53.28
1-aza,7-boracoronene	53.76
13-aza,16-boracoronene	53.76
13-aza,15-boracoronene	54.34
13-aza,3-boracoronene	55.70
1-aza,8-boracoronene	56.34
19-aza,21-boracoronene	56.36
19-aza,22-boracoronene	56.58
13-aza,5-boracoronene	57.13
13-aza,6-boracoronene	59.58

Table A2: Relative gibbs energies of the positional isomers obtained by two BN pair substitution to coronene.

Positional Isomers	Relative Energy (kcal/mol)
1,12-aza,2,13-boracoronene	0.00
1,19-aza,2,13-boracoronene	1.38
2,13-aza,1,19-boracoronene	3.83
2,13-aza,1,14-boracoronene	6.31

2,13-aza,1,12-boracoronene	8.90
1,5-aza,2,6-boracoronene	9.42
1,9-aza,2,10-boracoronene	9.42
1,6-aza,2,5-boracoronene	10.87
1,19-aza,13,20-boracoronene	10.91
1,10-aza,2,9-boracoronene	11.13
1,8-aza,2,7-boracoronene	11.24
1,7-aza,2,8-boracoronene	12.20
1,11-aza,2,12-boracoronene	12.57
14,19-aza,13,20-boracoronene	14.32
1,4-aza,2,15-boracoronene	17.49
13,20-aza,1,19-boracoronene	18.31
19,21-aza,13,20-boracoronene	22.65
1,5-aza,2,15-boracoronene	24.28
1,6-aza,2,16-boracoronene	25.39
19,21-aza,20,22-boracoronene	25.47
13,20-aza,19,21-boracoronene	26.45
1,15-aza,2,4-boracoronene	30.86
1,16-aza,2,6-boracoronene	31.26
1,15-aza,2,5-boracoronene	32.86

Table A3: Relative gibbs energies of the positional isomers obtained by the triple BN pair substitution to coronene.

Positional Isomers	Relative Gibbs Energy (kcal/mol)
1,14,19-aza,2,13,20-boracoronene	0.00
2,3,13-aza,1,4,14-boracoronene	13.11
1,12,19-aza,2,13,24-boracoronene	19.72
19,21,23-aza,20,22,24-boracoronene	23.75
1,12,14-aza,2,3,13-boracoronene	25.89
1,9,12-aza,2,10,13-boracoronene	26.03

1,5,12-aza,2,6,13-boracoronene	29.62
1,6,12-aza,2,5,13-boracoronene	31.55
1,10,12-aza,2,9,13-boracoronene	32.21
1,8,12-aza,2,7,13-boracoronene	33.74
1,3,12-aza,2,4,13-boracoronene	35.33
1,4,12-aza,2,3,13-boracoronene	35.49
1,7,12-aza,2,8,13-boracoronene	35.69
1,4,12-aza,2,13,15-boracoronene	36.15
1,12,19-aza,2,13,20-boracoronene	36.96
1,8,12-aza,2,13,17-boracoronene	38.70
1,7,12-aza,2,13,16-boracoronene	41.66
1,12,16-aza,2,7,13-boracoronene	46.10
1,5,12-aza,2,13,15-boracoronene	47.74
1,6,12-aza,2,13,16-boracoronene	47.84
1,12,17-aza,2,8,13-boracoronene	48.87
1,5,12-aza,2,6,13-boracoronene	49.18
1,12,15-aza,2,4,13-boracoronene	50.30
1,12,21-aza,2,13,22-boracoronene	51.02
1,12,20-aza,2,13,21-boracoronene	51.30
1,12,23-aza,2,13,22-boracoronene	51.89
1,12,22-aza,2,13,23-boracoronene	52.42
1,12,21-aza,2,13,20-boracoronene	52.64
1,12,23-aza,2,13,24-boracoronene	53.43
1,12,16-aza,2,6,13-boracoronene	53.64
1,12,19-aza,2,13,24-boracoronene	54.41
1,12,18-aza,2,10,13-boracoronene	55.08
1,12,15-aza,2,5,13-boracoronene	55.42
1,12,15-aza,2,13,24-boracoronene	57.18
1,12,22-aza,2,13,21-boracoronene	57.37
1,12,24-aza,2,6,23-boracoronene	59.41
1,12,17-aza,2,9,13-boracoronene	59.56

A4:

The relative stability of C=C w.r.t B=C is around 1.54 kcal calculated theoretically using isodesmic equation

